



Interaction between two graphene sheets with a turbostratic orientational relationship

Yasushi Shibuta^{a,*}, James A. Elliott^b

^aDepartment of Materials Engineering, The University of Tokyo, 7-3-1 Hongo, Bunkyo-ku, Tokyo 113-8656, Japan

^bDepartment of Materials Science and Metallurgy, University of Cambridge, Pembroke Street, Cambridge CB2 3QZ, UK

ARTICLE INFO

Article history:

Available online 13 July 2011

ABSTRACT

The interaction of two rigid defect-free graphene sheets with various turbostratic orientational relationships is examined using a Lennard-Jones potential. When one layer is rotated from the AB stacking order, maxima and minima in the potential energy occur at angles corresponding to AA and AB stacking. The energy gap between AA and AB stacking is estimated to be much smaller than the average thermal energy at room temperature. Turbostratic orientations diminish the energy for translational displacement to zero. The presence of defects is required to explain non-zero shear strengths in pure carbon nanotube fibres with no commensurate orientation of graphene sheets.

© 2011 Elsevier B.V. All rights reserved.

1. Introduction

The mechanical properties of carbon nanotubes (CNTs) [1] have been studied extensively using both experimental [2–5] and theoretical [6–10] approaches, since it is anticipated that they will enable the development of advanced materials such as ultrahigh strength CNT fibres [11–17]. However, the mechanical properties of pure CNT fibres depend not only on the quality of the constituent CNTs, but also on the interaction between individual CNTs and bundles within the fibre. Therefore, many researchers have focused on the cohesion and stress transfer between graphene layers within multiwall carbon nanotubes (MWCNTs) and those between neighbouring CNTs in the fibre in order to understand the origin of CNT fibre strength [17–22]. In particular, Vilatela and coworkers [17] recently derived a model to explain the strength of CNT fibres on the basis of continuum elasticity theory, molecular mechanics and image analysis of transmission electron micrographs. They highlighted four factors which currently limit the strength of CNT fibres made up of fibrous elements: (i) the fraction of the total number of graphene layers that are on the outside of the fibrous element, (ii) the fraction of the surface of the outer graphene wall of the element in contact with neighbouring elements, (iii) the mean length of constituent CNTs and (iv) the shear strength between graphene sheets. The first factor is geometric in origin, that is, the ratio of the outer graphene surface, which contributes to the interaction with neighbouring elements, increases with decreasing number of layers of the constituent CNTs. With respect to the second factor, CNTs polygonized under pressure [17–19] and by twisting [20] have been shown to enhance the stress transfer between

CNTs due to the increase in contact area. The correlation between the fibre strength and CNT length is shown in the summary of data from various literatures [17], although there is no similar correlation for the fibre stiffness.

The shear stress between adjacent graphene layers, which is the last factor among those listed above, has been measured experimentally and calculated by simulations. The range of the measured and calculated values is very wide: from 0.04 [21] to 69.0 [22] MPa depending on methodology used (see Table 1 in Ref. [17]). As discussed in Ref. [17], the ambiguous concept of shear strength for graphene layers compared to bulk materials makes the estimation of the shear stress of graphite layers difficult. For example, Kolmogorov and Crespi [23] found that cancellation of registry-dependent interactions in incommensurate CNTs and certain axially commensurate CNTs leads to a shear strength that is independent of nanotube length. Furthermore, experimentally measured shear strengths depend greatly on the condition of the graphene surface. Suekane et al. [22] revealed that the shear strength of 40 MPa for as-synthesized CNTs decreased dramatically to 2 MPa after annealing of CNTs to obtain a clean graphene surface. The orientational relationship between graphene layers is another important factor that may affect the strength of the graphene intersheet interface. Saito and co-workers [24] calculated the interlayer interaction in double wall carbon nanotubes (DWCNTs) with various combinations of chiral angles using a Lennard-Jones potential, and found that the stability of DWCNTs does not depend on the relative chiral angle of inner and outer layers, but on the diameter difference between them. Shibuta and Maruyama [25] performed molecular dynamics (MD) simulation of generation process of DWCNTs from a peapod (a CNT encapsulating C₆₀ molecules) by heat treatment and showed the chiral angle of the inner tube generated by the heat treatment was not dependent on that of the outer tube but

* Corresponding author. Fax: +81 3 5841 8653.

E-mail address: shibuta@material.t.u-tokyo.ac.jp (Y. Shibuta).

on the diameter. On the other hand, Bichoutskaia et al. [26] performed DFT calculations of interwall interactions in DWCNTs, and found axial shear strengths between 4 and 215 MPa depending on the relative diameters and chiral angles of inner and outer tubes. Moreover, the orientational relationship between graphene network and the surface of transition metals is also important, and may be a key factor determining the chiral angle of CNTs made by catalytic chemical vapour deposition [27–30].

It is well known that the AB stacking order between graphene layers in graphite is energetically stable [31,32]. However, there is little information on the interaction between the graphite layers with a turbostratic orientational relationship, which is often observed in the interlayer interaction of individual MWCNTs and the interaction between neighbouring CNTs in a CNT fibre. Lebedeva et al. [33] have recently put forward a fast diffusion mechanism for a graphene flake on an infinite graphene layer in which there is a rotational transition from a commensurate to incommensurate state, with subsequent rotation and translation until a commensurate state is again reached. They proposed that at temperatures exceeding the barrier for transitions between commensurate states, the main contribution to translational motion is from the incommensurate states, and recently estimated a critical unit elongation for the formation of an incommensurability defect of just 0.39% along the armchair direction [34]. Hence, the interaction between graphene sheets with turbostratic orientational relationship is examined systematically in this Letter. After briefly summarizing the simulation methodology in Section 2, the interaction energies of two graphene layers as a function of rotation angle from the AB stacking order are examined in Section 3.1. Then, the interaction energies of two graphene sheets as a function of translational displacement from the AB stacking order and various turbostratic structures are examined in Section 3.2. We conclude with a discussion of the implications of these results for the shear stress transfer in CNT fibres, including some suggestions for improving this limiting factor in determining their strength.

2. Simulation methodology

The interaction energy of two perfectly rigid graphene sheets ($a = 1.42 \text{ \AA}$, where a is the bond length between carbon atoms) with various orientation relationships are examined using a standard 12–6 Lennard-Jones (LJ) potential between pairs of atoms with separation r :

$$E(r) = 4\epsilon \left\{ \left(\frac{\sigma}{r} \right)^{12} - \left(\frac{\sigma}{r} \right)^6 \right\} \quad (1)$$

The parameters $\epsilon = 2.168 \text{ meV}$ ($3.474 \times 10^{-22} \text{ J}$) and $\sigma = 3.36 \text{ \AA}$ were employed for describing the van der Waals potential between graphene sheets per atom, which are fitted to reproduce the interlayer distance in graphite as 3.35 \AA [17]. We note that there are various parameter sets available to describe the LJ potential between graphene sheets. For example, Saito et al. [24] employed the parameters of the LJ potential, $\epsilon = 2.968 \text{ meV}$ and $\sigma = 3.407 \text{ \AA}$, which produces an interlayer separation of 3.354 \AA and an elastic constant $C_{33} = 4.08 \text{ GPa}$ for graphite, to calculate the potential barrier for the relative displacement of the inner and outer layer for a DWNT. Moreover, Shibuta and Maruyama have employed the parameters of the LJ potential, $\epsilon = 2.50 \text{ meV}$ and $\sigma = 3.37 \text{ \AA}$, which were used for fitting the interaction energy of periodic graphene sheets to the one-dimensional averaged LJ potential [25]. Therefore, we have investigated the dependence of the interaction energy on the potential parameters in Section 3.1. Since our focus is on graphene sheets with a turbostratic orientational relationship, we neglect any energy term that results from interlayer delocalisation of π orbitals in AB graphite [32].

The interaction energy between two graphene sheets with various orientation relationships is calculated as follows. A fixed graphene sheet with 1560 carbon atoms, consisting of 15 armchair \times 26 zigzag unit lengths, is placed parallel to the x – y plane in a cubic cell under the periodic boundary conditions. The bond length between carbon atoms in graphene sheets is set to be 1.42 \AA . Then, a movable graphene sheet with 336 carbon atoms consisting of 7 armchair \times 12 zigzag unit lengths is placed parallel to the fixed sheet with an intersheet distance in the range of 3.25 – 3.45 \AA . The movable graphene sheet is rotated or translated while being maintained parallel to the fixed graphene sheet. The interaction energy per atom is calculated as the total interaction energy divided by the total number of atoms. The effect of the edge in the movable graphene sheet is negligible since the ratio of the edge atoms to all atoms considered is small enough.

3. Results and discussion

3.1. Interaction energy of graphene sheets with respect to rotation angle

First, the interaction energy of two graphene sheets as a function of rotation angle from AB stacking order was examined. There are two unique rotation axes reproducing rotational displacements from the AB stacking order: one passing through a carbon atom in each of the two sheets (Figure 1a) and the other passing through a carbon atom in one layer and a hollow site in the other sheet (Figure 1b). When one sheet is rotated with respect to the axis passing through an atom in each of the two sheets, the AA and AB stacking orders appear alternately via turbostratic structures with a period of 60° (Figure 1a). On the other hand, only the AB stacking order appears with a period of 60° in the case of the axis passing through one atom and hollow site (Figure 1b). Figure 2 shows the interaction energy of two graphene sheets with a separation of 3.35 \AA as a function of rotation angle with respect to two axes mentioned above. Maxima and minima in the rotational potential energy surface were found alternately at an angle corresponding to the AA and AB stacking orders in the case of the axis penetrating two atoms, whereas only minima appeared at an angle corresponding to the AB stacking order for the other axis. The interaction energies of two graphene sheets at the AA and AB stacking orders were -17.36 and $-17.72 \text{ meV atom}^{-1}$ respectively, which, when multiplied by a factor of two, compare well with the binding energy in graphite ($-40 \text{ meV atom}^{-1}$ [35] and collapsed CNTs ($-35 \text{ meV atom}^{-1}$) [36]. The energy gap between the AA and AB stacking orders is just $0.36 \text{ meV atom}^{-1}$, which is an underestimate due to the neglect of delocalisation energy in the AB structure, but is comparable in magnitude to that calculated by Lebedeva et al. ($1.1 \text{ meV atom}^{-1}$) [33] for flexible sheets bound by a Brenner potential [37]. Hence, the two graphene sheets have the possibility for relative rotational motion at room temperature (cf. $k_B T = 25.7 \text{ meV atom}^{-1}$ at $T = 298 \text{ K}$, where k_B is the Boltzmann constant). No significant difference in the interaction energy was found for any turbostratic structures, which is almost constant at $-17.61 \text{ meV atom}^{-1}$ on average. The interaction energies as a function of rotation angle calculated with different parameter sets of the LJ potential: $\epsilon = 2.968 \text{ meV}$ and $\sigma = 3.407 \text{ \AA}$ from Ref. [24], and $\epsilon = 2.50 \text{ meV}$ and $\sigma = 3.37 \text{ \AA}$ from Ref. [25] are provided in the Supplementary material. It was confirmed that the interaction energy as a function of rotation angle behaves in the same manner for all the parameter sets and only the magnitude of the interaction energy differs corresponding to the depth of the potential. By comparison, the energy gaps between the AA and AB stacking orders calculated with various depths of the LJ potential, $\epsilon = 2.168$ (this study), 2.5 [25] and 2.968 meV [24] are 0.36 , 0.43 and

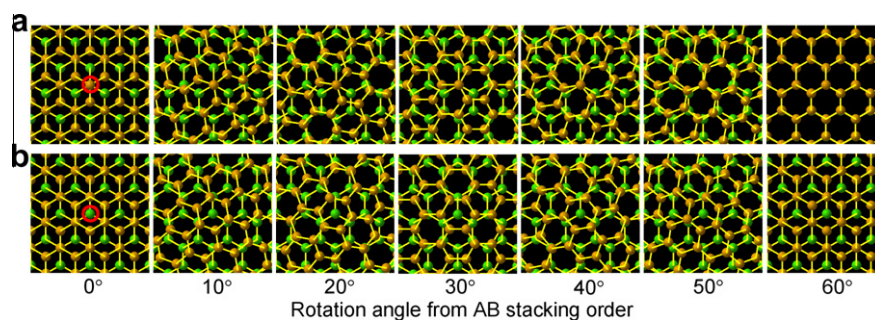


Figure 1. Orientational relationships in two graphene sheets as a function of rotation angle from the AB stacking order with respect to two axes (encircled by red circles): (a) the axis penetrating two carbon atoms on each of the two layers and (b) the axis penetrating one atom in one layer and a hollow site in the other layer. Orange and green atoms represent carbon atoms belonging to upper and lower graphene sheets, respectively. (For interpretation of the references to colour in this figure legend, the reader is referred to the web version of this article.)

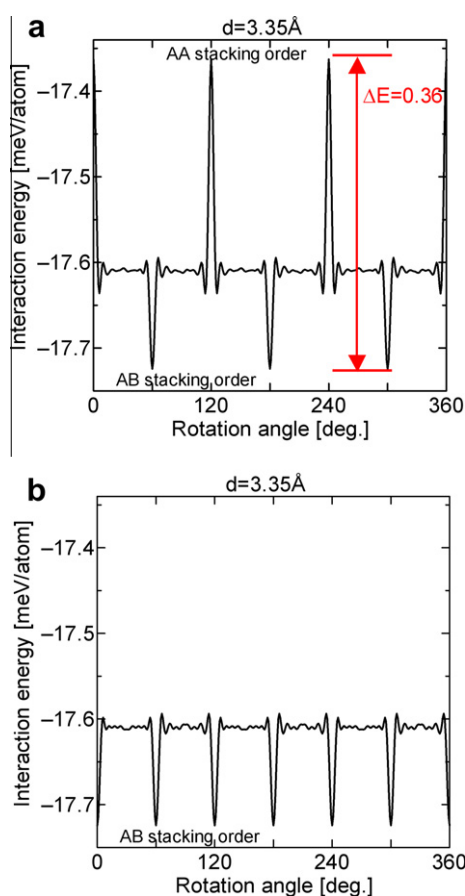


Figure 2. Interaction energy of two graphene sheets with 3.35 Å spacing as a function of rotation angle from the AB stacking order with respect to two axes corresponding to the axes shown in Figure 1. The energy gap between the AA and AB stacking orders is indicated by the arrowed line.

0.59 meV atom⁻¹, respectively. Since there is no significant difference in the trend of the interaction energy among parameter sets except for the magnitude, only one parameter set is employed in the following calculations.

In addition, the interaction between two graphene sheets with respect to the interlayer distance was examined. Here, the interaction energy at the AA and AB stacking orders and a turbostratic structure, which is intermediate in rotation angle between the AA and AB stacking orders, was calculated for the interlayer distance in the range of 3.25–3.45 Å with an interval of 0.1 Å. Figure 3 shows the interaction energies of the two graphene sheets with the

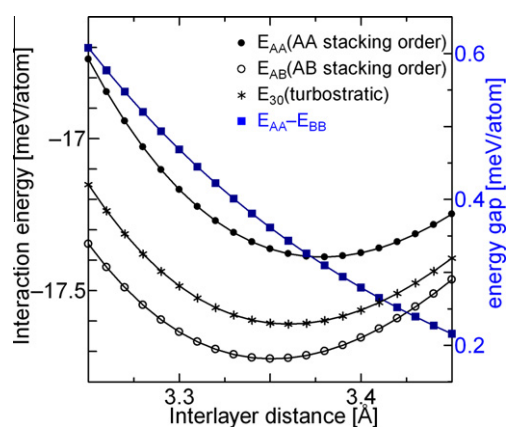


Figure 3. Interaction energy of two graphene sheets with the AA and AB stacking orders and the turbostratic structure (the middle structure between AA and AB stacking orders) as a function of interlayer distance. The energy gap between the AA and AB stacking orders are also plotted.

AA and AB stacking orders and a turbostratic structure (30° rotated from the AB stacking) as a function of interlayer distance. The energy gap between the AA and AB stacking orders are also plotted. The interaction energy of the AB stacking orders was the lowest among all orientations considered at every interlayer distance and that of the AA stacking was the highest. The interlayer distance with the lowest interaction energy slightly increased with increasing the rotation angle from the AB stacking order: 3.35 Å for the AB stacking order, 3.36 Å for the turbostratic structure and 3.38 Å for the AA stacking order, respectively. The energy gap between the AA and AB stacking orders increased monotonically with decreasing the interlayer distance, the magnitude of which is less than 1 meV atom⁻¹ in the range considered. Hence, it was confirmed that two graphene sheets with any orientational relationship have easy rotational motion around the equilibrium interlayer distance at room temperature.

3.2. Interaction energy of graphene sheets with respect to translational displacement

Next, the interaction energy of two graphene sheets as a function of translational displacement was examined, starting from the AB stacking order. The unit lengths of the graphene with respect to the zigzag (x -axis in Figure 4a) and the armchair direction (y -axis in Figure 4a) are $\sqrt{3}a$ and $3a$, respectively, where a is the equilibrium bond length between carbon atoms. When one layer is translated parallel to the armchair direction (y -axis) from the AB stacking order, other AB stacking and AA stacking orders appear

during translation over one unit length. On the other hand, neither AA nor AB stacking orders appear during translation parallel to the zigzag direction (x -axis) over one unit length. Figure 4b shows the interaction energy of two graphene sheets with 3.35 Å separation as a function of translational displacement with respect to two orthogonal directions indicated in Figure 4a. The interaction energies at the AA and AB stacking orders were the same as the ones calculated in the Figure 2. Two different energy barriers were found between AB stacking orders appearing depending on the translation direction: the energy barrier during the translation in the zigzag direction, $0.15 \text{ meV atom}^{-1}$, was higher than that for the armchair direction, $0.03 \text{ meV atom}^{-1}$. The difference in the energy barrier depending on the translational direction may cause anisotropy in the mobility of the graphene sheets, although the magnitude of both energy barriers is much smaller than the average thermal energy at room temperature.

Moreover, the interaction energy of two graphene sheets with respect to the translational displacement starting from various turbostratic structures was examined, which has not been examined systematically in the past to the best of our knowledge. The interaction energy for the turbostratic structures was calculated as follows. First, initial turbostratic structure were prepared by rotating one layer of the AB stacking order with respect to the axis one atom and hollow site (Figure 1b) for various rotation angles. The various rotation angles were chosen within one symmetric period (60°) as $1^\circ, 2^\circ, 3^\circ, 4^\circ, 5^\circ, 10^\circ, 20^\circ, 30^\circ, 40^\circ, 50^\circ, 55^\circ, 56^\circ, 57^\circ, 58^\circ$ and 59° . The interlayer distance was set to be 3.35 Å. The prepared structures were then translated with respect to both the x - and y -axis direction for one unit length as same as previous calculation shown in Figure 4. Figure 5 shows the interaction energy as a function of translational displacement with respect to two orthogonal directions. When the initial structure was rotated a few degrees from the AB stacking, the difference in the interaction energy between the maximum and minimum dropped abruptly and the interaction energy became almost constant with respect to translating displacement for the initial turbostratic structures with the rotation

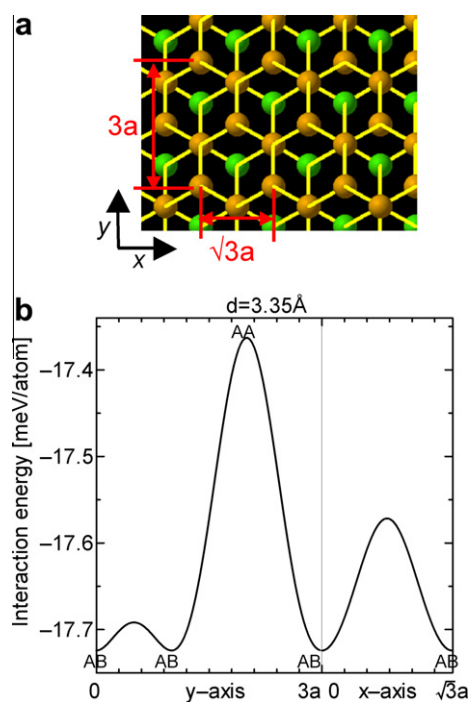


Figure 4. (a) Unit lengths of the graphite network with respect to zigzag (x -axis) and armchair (y -axis) directions. (b) Interaction energy of two graphene sheets with 3.35 Å spacing as a function of translational displacement starting from the AB stacking order with respect to the x - and y -axis directions.

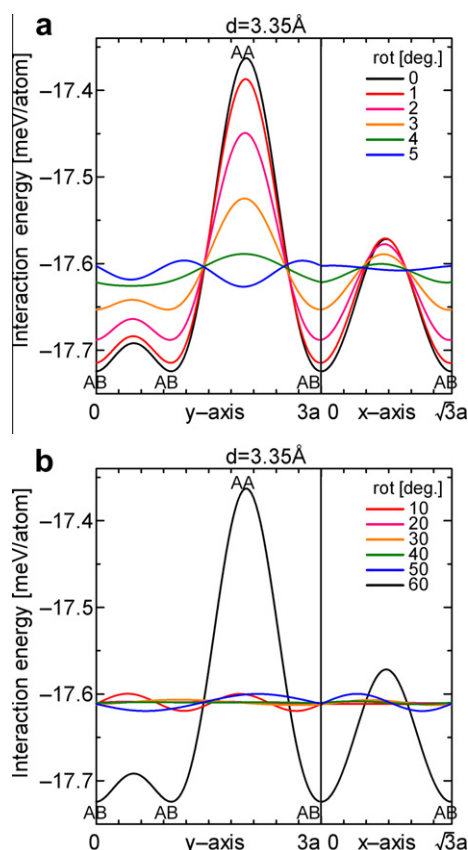


Figure 5. Interaction energy of two graphene sheets with 3.35 Å spacing as a function of translational displacement with respect to the directions for x - and y -axis starting from various turbostratic structures: (a) the initial turbostratic structure with rotation angles of 0–5° and (b) 10–60° from the AB stacking order.

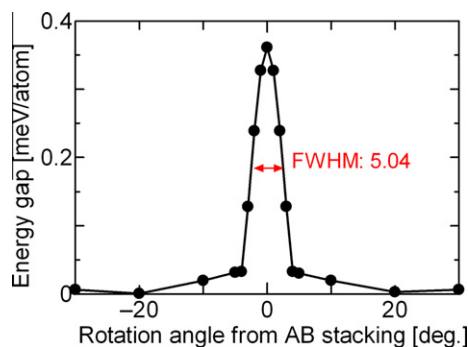


Figure 6. Energy gaps in the interaction energy of two graphene sheets obtained by the translational displacement of turbostratic structures with various rotation angles from the AB stacking order. Full width at half maximum (FWHM) is indicated by the arrowed line.

angle between 5° and 55° . Figure 6 shows the energy gaps during translational displacement for various turbostratic structures, which are defined from the energy difference between the maximum and minimum of the interaction energy during the translational displacement. As shown in Figure 5, a few degrees rotation from the AB stacking diminished the energy gap abruptly. The full width at half maximum (FWHM) is 5.04° , which means the slight rotational displacement from the AB stacking order diminishes the energy gap with respect to translation of the graphene sheets effectively to zero. This implies that the contribution of van der Waals interactions to shear strength in CNT fibres will be negligible if the areas of graphene sheet in contact are perfectly rigid,

defect-free and with a turbostratic arrangement between CNTs. Thus, the presence of defects or covalent cross-links between real materials is inferred from their non-zero (but small) shear strengths measured in experiment.

4. Conclusions

The interaction energy of the two rigid defect-free graphene sheets with respect to rotation angle and translational displacement was examined using a standard 12–6 Lennard-Jones potential. When one layer was rotated from the AB stacking order, maxima and minima in the potential energy surface occurred periodically at angles corresponding to the AA and AB stacking orders. The energy gap between the AA and AB stacking orders was 0.36 meV atom⁻¹, and increased with decreasing interlayer separation. However, the interaction energy was much smaller than the average thermal energy at room temperature ($k_B T = 25.7$ meV atom⁻¹) in the range examined. This implies that two graphene sheets will have easy rotational motion around equilibrium interlayer separation at room temperature. When the one layer was translated from the AB stacking order, two different energy barriers between the AB stacking order appeared depending on the direction of translation, both of which were also much smaller than the average thermal energy at room temperature. In addition, the translational displacement of the turbostratic structure showed that a few degrees rotation from the AB stacking order diminished the energy gap abruptly, with a FWHM of just 5.04°.

In this study, the interaction energy of two graphene sheets with a turbostratic orientational relationship was examined using rigid defect-free graphene sheets for simplicity, which results in much smaller interaction energy than average thermal energy at room temperature. However, for real materials with finite in-plane compressibility, out-of-plane distortions or containing defects, the interaction between graphene sheets may be much larger. This is consistent with aforementioned experimental report by Suekane et al. [22] that the shear strength of as-synthesized CNTs of 40 MPa decreased dramatically to 2 MPa after annealing of CNTs to obtain a clean graphene surface. In fact, the existence of the defects may strengthen the interaction of graphene sheets in shear due to the interlayer carbon covalent bonds, which are newly generated by the dangling bonds around the defects, whereas only van der Waals interactions are considered in this study. In addition, the existence of the defects may lower the in-plane stiffness of the graphene sheets, which may result in an increase of the shear stress transfer due to a reduction in the distance between stacking fault dislocations in the graphene sheets [38]. The interaction energy including the effect of defects will be examined in future work.

Acknowledgements

The authors would like to thank Dr. Juan J. Vilatela and Prof. Alan H. Windle at University of Cambridge for fruitful discussions. Y.S. gratefully acknowledges Japan Society for Promotion of

Science (JSPS) for funding of the Institutional Program for Young Researcher Overseas Visits, held at University of Cambridge. Part of this research was supported by the Grant-in-Aid for Young Scientists (a) (No. 21686021) from Ministry of Education, Culture, Sports, Science and Technology (MEXT), Japan.

Appendix A. Supplementary data

Supplementary data associated with this article can be found, in the online version, at doi:10.1016/j.cplett.2011.07.013.

References

- [1] S. Iijima, *Nature* 354 (1991) 56.
- [2] E.W. Wong, P.E. Sheehan, C.M. Lieber, *Science* 277 (1997) 1971.
- [3] D.A. Walters, L.M. Ericson, M.J. Casavant, J. Liu, D.T. Colbert, K.A. Smith, R.E. Smalley, *Appl. Phys. Lett.* 74 (1999) 3803.
- [4] M.-F. Yu, O. Lourie, M.J. Dyer, K. Moloni, T.F. Kelly, R.S. Ruoff, *Science* 287 (2000) 637.
- [5] Y. Nakayama, *Jpn. J. Appl. Phys.* 46 (2007) 5005.
- [6] B.I. Yakobson, C.J. Brabec, J. Bernholc, *Phys. Rev. Lett.* 76 (1996) 2511.
- [7] J.P. Lu, *Phys. Rev. Lett.* 79 (1997) 1297.
- [8] H. Mori, Y. Hirai, S. Ogata, S. Akita, Y. Nakayama, *Jpn. J. Appl. Phys.* 44 (2005) L1307.
- [9] S. Inoue, Y. Matsumura, *Chem. Phys. Lett.* 469 (2009) 125.
- [10] H. Deguchi, Y. Yamaguchi, K. Hirahara, Y. Nakayama, *Chem. Phys. Lett.* 503 (2011) 272.
- [11] Y.-L. Li, I.A. Kinloch, A.H. Windle, *Science* 304 (2004) 276.
- [12] K. Kozioł, J. Vilatela, A. Moissala, M. Motta, P. Cuniff, M. Sennett, A. Windle, *Science* 318 (2007) 1892.
- [13] M. Motta, A. Moissala, I.A. Kinloch, A.H. Windle, *Adv. Mater.* 19 (2007) 3721.
- [14] X. Zhang et al., *Adv. Mater.* 19 (2007) 4198.
- [15] N. Behabtu, M.J. Greena, M. Pasquali, *Nano Today* 3 (2008) 24.
- [16] J.J. Vilatela, A.H. Windle, *Adv. Mater.* 22 (2010) 4959.
- [17] J.J. Vilatela, J.A. Elliott, A.H. Windle, *ACS Nano* 5 (2011) 1921.
- [18] J.A. Elliott, J.K.W. Sandler, A.H. Windle, R.J. Young, M.S.P. Shaffer, *Phys. Rev. Lett.* 92 (2004) 095501.
- [19] X. Zhang, Q. Li, *ACS Nano* 4 (2009) 312.
- [20] D. Qian, W.K. Liu, R.S. Ruoff, *Compos. Sci. Technol.* 63 (2003) 1561.
- [21] A. Kis, K. Jensen, S. Aloni, W. Mickelson, A. Zettl, *Phys. Rev. Lett.* 97 (2006) 025501.
- [22] O. Suekane, A. Nagataki, H. Mori, Y. Nakayama, *Appl. Phys. Exp.* 1 (2008) 064001.
- [23] A.N. Kolmogorov, V.H. Crespi, *Phys. Rev. Lett.* 85 (2000) 4727.
- [24] R. Saito, R. Matsuo, T. Kimura, G. Dresselhaus, M.S. Dresselhaus, *Chem. Phys. Lett.* 348 (2001) 187.
- [25] Y. Shibuta, S. Maruyama, *Heat Transfer-Asian Res* 35 (2006) 254.
- [26] E. Bichoutskaia, O.V. Ershova, Y.E. Lozovik, A.M. Popov, *Tech. Phys. Lett.* 35 (2009) 666.
- [27] Y. Shibuta, S. Maruyama, *Chem. Phys. Lett.* 382 (2003) 381.
- [28] Y. Shibuta, J.A. Elliott, *Chem. Phys. Lett.* 427 (2006) 365.
- [29] Y. Shibuta, J.A. Elliott, *Chem. Phys. Lett.* 472 (2009) 299.
- [30] Y. Shibuta, *Diamond Relat. Mater.* 20 (2011) 334.
- [31] J.D. Bernal, *Proc. R. Soc. London, Ser. A* 106 (1924) 749.
- [32] J.-C. Charlier, X. Gonze, J.-P. Michenaud, *Europhys. Lett.* 28 (1994) 403.
- [33] I.V. Lebedeva, A.A. Knizhnik, A.M. Popov, O.V. Ershova, Y.E. Lozovik, B.V. Potapkin, *Phys. Rev. B* 82 (2010) 155460.
- [34] A.M. Popov, I.V. Lebedeva, A.A. Knizhnik, Y.E. Lozovik, B.V. Potapkin, *Phys. Rev. B* 84 (2011) 045404.
- [35] L.A. Girifalco, R.A. Ladd, *J. Chem. Phys.* 25 (1956) 693.
- [36] L.X. Benedict, N.G. Chopra, M.L. Cohen, A. Zettl, S.G. Louie, V.H. Crespi, *Chem. Phys. Lett.* 286 (1998) 490.
- [37] D.W. Brenner, O.A. Shenderova, J.A. Harrison, S.J. Stuart, B. Ni, S.B. Sinnott, *J. Phys.: Condens. Matter* 14 (2002) 783.
- [38] R.H. Telling, M.I. Heggie, *Philos. Mag. Lett.* 83 (2003) 411.